Lab on a Chip

Accepted Manuscript

This is an *Accepted Manuscript*, which has been through the Royal Society of Chemistry peer review process and has been accepted for publication.

Accepted Manuscripts are published online shortly after acceptance, before technical editing, formatting and proof reading. Using this free service, authors can make their results available to the community, in citable form, before we publish the edited article. We will replace this *Accepted Manuscript* with the edited and formatted *Advance Article* as soon as it is available.

You can find more information about *Accepted Manuscripts* in the Information for Authors.

Please note that technical editing may introduce minor changes to the text and/or graphics, which may alter content. The journal's standard Terms & Conditions and the Ethical guidelines still apply. In no event shall the Royal Society of Chemistry be held responsible for any errors or omissions in this *Accepted Manuscript* or any consequences arising from the use of any information it contains.

ROYAL SOCIETY OF CHEMISTRY

www.rsc.org/loc

ARTICLE TYPE www. rsc.org/xxxxxx | XXXXXXXX

Microfluidic immunocapture of circulating pancreatic cells using parallel EpCAM and MUC1 capture: characterization, optimization and downstream analysis†

Fredrik I. Thege,[a] Timothy B. Lannin,[b] Trisha N. Saha,[c,d] Shannon Tsai,[c], Michael L. Kochman,[c] Michael A. Hollingsworth,[e] Andrew D. Rhim,[c,d] and Brian J. Kirby[b,f]

Received Xth XXXXXXXXXX 20XX, Accepted Xth XXXXXXXXX 20XX
First published on the web Xth XXXXXXXXXX 200X
DOI: 10.1039/b000000x

We have developed and optimized a microfluidic device platform for the capture and analysis of circulating pancreatic cells (CPCs) and pancreatic circulating tumor cells (CTCs). Our platform uses parallel anti-EpCAM and cancer-specific mucin 1 (MUC1) immunocapture in a silicon microdevice. Using a combination of anti-EpCAM and anti-MUC1 capture in a single device we are able to achieve efficient capture while extending immunocapture beyond single marker recognition. We also detect a known oncogenic KRAS mutation in cells spiked in whole blood using immunocapture, RNA extraction, RT-PCR and Sanger sequencing. To allow for downstream single-cell genetic analysis, intact nuclei were released from captured cells by use of targeted membrane lysis. We have developed a staining protocol for clinical samples, including standard CTC markers; DAPI, cytokeratin (CK) and CD45, and a novel marker of carcinogenesis in CPCs, mucin 4 (MUC4). We also demonstrate a semi-automated approach to image analysis and CPC identification, suitable for clinical hypothesis generation. Initial results from immunocapture of a clinical pancreatic cancer patent sample show that parallel capture may capture more of the heterogeneity of the CPC population. With this platform we aim to develop a diagnostic biomarker for early pancreatic carcinogenesis and patient risk stratification.

Background and introduction

Pancreatic cancer (PC), the fourth leading cause of cancer-related death in the US is associated a poor 5-year patient survival rate of less than 5%. PC is characterized by rapid and often symptom-free progression, resulting in more than 90% of patients being diagnosed with metastatic disease[1], a stage at which there are no effective treatment options. Clinical data show that the treatment outcome improves dramatically if PC is caught at an early stage, prior to the formation of clinically-detectable metastasis.[1 2] Early detection is thus the most efficient way to improve overall patient survival, but detection is limited by the absence of specific clinical biomarkers and non-invasive screening tests.[2]

The formation of metastasis is attributed to the intravasation of cells from the primary site of disease into the blood stream, followed by transport to a secondary site where the cells extravasate, proliferate and form secondary lesions.[3 4 5] These cells are in general referred to as circulating tumor cells (CTCs). Here, we refer to any cell that disseminates from the pancreas into the blood stream as a circulating pancreatic cell (CPC). Recent results in a mouse model that recapitulates human pancreatic carcinogenesis have shown that dissemination of cells from the pancreas occurs prior to tumor formation[6]. Furthermore, we have recently shown that epithelial pancreatic cells can be found in the circulation of patients with pancreatic cyst lesions in the absence of overt tumor formation, making CPCs a more appropriate term for this cell population.[7] In future studies, early dissemination of CPCs could thus offer partial explanation to the rapid and aggressive progression observed in PC patients. Precancerous CPC dissemination also allows for the development of early detection biomarkers of pancreatic carcinogenesis.

CTCs have been shown to be prognostic of patient survival in a number of cancers and are suggested to be of disease

[a] *Department of Biomedical Engineering, College of Engineering, Cornell University, Ithaca, NY 14853, USA; E-mail: fit5@cornell.edu*
[b] *Sibley School of Mechanical & Aerospace Engineering, College of Engineering, Cornell University, Ithaca, NY 14853, USA*
[c] *Gastroenterology Division, Department of Medicine, University of Pennsylvania, Philadelphia, PA 19104, USA*
[d] *Division of Gastroenterology, Department of Internal Medicine, University of Michigan School of Medicine, Ann Arbor, MI 48109*
[e] *Eppley Institute for Research in Cancer and Allied Diseases, University of Nebraska Medical Center, Omaha, NE 68198*
[f] *Division of Hematology/Oncology, Department of Medicine, Weill Cornell Medical College, New York, NY 10065, USA*
† Electronic Supplementary Information (ESI) available: [details of any supplementary information available should be included here]. See DOI: 10.1039/b000000x/

Lab on a Chip Accepted Manuscript

mechanistic importance and of diagnostic value.[8] The extreme rarity of CTCs in peripheral circulation makes CTC isolation technically challenging. To allow for their efficient isolation, a range of microfluidic platforms have been developed.[9] These platforms have explored a range of physical principles and geometries to achieve efficient and pure isolation, including; micropillar arrays[10,11,12], vortex-inducing microgrooves[13], microsieves and filters,[14,15] magnetic microbeads[16] and inertial separation[17]. Some techniques rely solely on passive separation of CTCs based on physical parameters such as cell size and stiffness. However, a majority of techniques use an optimized surface capture chemistry to achieve CTC isolation. Immunocapture using surface functionalization of capture antibodies has emerged as the dominant technique for isolating CTCs in microfluidic devices[9] and relies on the collision of target cells with a immunofunctionlized surface. In these devices, the geometry serves to maximize the interaction of target cells with the capture chemistry. We have previously described one such geometry[11,18], that maximizes the cell-capture surface interaction of larger cells, such as CTCs, in combination with an optimized CTC capture chemistry. The choice of capture chemistry influences the resulting population of captured cells and needs to be optimized for each application and disease studied. Antibodies for different cancer and epithelial markers, such as epithelial cell adhesion molecule (EpCAM)[7,10], prostate specific membrane antigen (PSMA)[11,18], Her2[19,20] and EGFR[20] have been used to capture CTCs from a range of cancers. Due to their inherent difference in specificity and binding affinity the choice of antibody clone has been shown to dominate capture performance.[21] In the case of prostate cancer, the use of the tissue specific marker PSMA has been shown to result in superior capture as compared to capture using the commonly used marker EpCAM.[18] The capture chemistry should thus ideally be optimized for each specific application and for a specific cancer type. Here we aim to show that using recognition of a combination two markers, both upregulated in PC we can achieve efficient CPC capture. We also aim to show that the choice of capture chemistry governs the phenotype of captured cells.

As previously stated, EpCAM is the most widely used target for immunocapture of CTCs.[10,13,22,11] However, there is mounting evidence that EpCAM is downregulated in CTCs from some clinical samples[20] and during the cancer-associated process referred to as Epithelial-to-Mesenchymal Transition (EMT)[3], making EpCAM capture alone a potential source of bias for the capture of CPCs. In cancerous and precancerous tissues, EMT results in the development of an invasive phenotype[6,23,24] and has been shown to correlate with cancer progression.[20] On a cellular level, EMT results in the loss of epithelial markers and an upregulation of mesenchymal markers, as well as a gross change in cell morphology.[6,23] Furthermore, because recent PC mouse model data indicate the a vast majority of CPCs display an EMT phenotype, anti-EpCAM capture alone may fail to capture this potentially clinically significant CPC subpopulation. Breast cancer patient CTCs have been shown to express a dynamic range of EMT composition in a way that correlates with treatment outcome.[20] There is thus a pressing need to find alternative and/or complementary, EMT-robust capture modes. In this study we explore parallel anti-EpCAM and anti-mucin capture as a promising novel capture chemistry.

Mucins are a family of high-molecular-weight glycoproteins that are expressed by epithelial tissues, such as the respiratory and gastric linings as well as the ducts of the liver and pancreas, where they protect and lubricate the surfaces.[25] The founding member of this protein family, mucin 1 (MUC1) is expressed at a low level in healthy pancreas tissue, but has been shown to be strongly upregulated in pancreatic carcinogenesis[25,26]. Furthermore, overexpression of MUC1 has been shown to increase cancer cell invasiveness and motility through the induction of EMT in a PC mouse model.[27] MUC1 expression in CTCs from metastatic pancreatic patients has also been associated with shorter median overall patient survival.[28] The cancer-associated post-translational modification of MUC1 differs significantly from MUC1 found in healthy tissues.[29] Cancer-associated MUC1 is typically aberrantly hypoglycosylated[30,31] and the loss of cell polarity that occurs during carcinogenesis results in expression of MUC1 uniformly covering the cell membrane rather than being restricted to the apical side of the epithelial cell[31]. Furthermore, the aberrant expression pattern and hypoglycosylation of MUC1 exposes regions of the protein backbone to antibody binding, allowing for the creation of cancer-specific antibodies that bind minimally to MUC1 from healthy tissues[30,31]. An antibody specific to hypoglycosyled MUC1 (hMUC1) has previously been shown to induce cell adhesion when functionalized to the surface in a E-selectin cell-rolling assay.[32] Although MUC1 has been observed on the surface of some activated T-cells[33], the MUC1 expression level is low and of a distinct glycoform[34], making hMUC1 cancer cell specific in blood samples. Together, the strong upregulation, cancer-specific hypoglycosylation and change in spatial distribution, make hMUC1 an ideal target for the capture of CPCs in early carcinogenesis, allowing for the exploration of the link between capture chemistry and resulting phenotype of early disseminated CPCs.

The clinical implementation of a CPC capture platform relies on the specific and robust identification of captured CPCs and rejection of contaminating leukocytes. Cytokeratin (CK) is an epithelial marker that is frequently used as a positive marker of CTCs.[10] However, CK has in patient samples been shown to be downregulated more than EpCAM during EMT.[35] Mucin 4 (MUC4) has been shown to be differ-

Lab on a Chip Accepted Manuscript

This journal is © The Royal Society of Chemistry [year]

entially upregulated in pancreatic carcinogenesis; MUC4 is not expressed by healthy pancreatic tissues but strongly upregulated in cancerous and precancerous neoplastic pancreatic lesions[29 36 37]. Since CK expression may be lost during pancreatic carcinogenesis, we suggest using CK and MUC4 as orthogonal positive indicators of CPC identity. The relationship between CK and MUC4 expression level in the CPC population may also be an indicator of the EMT state of the CPCs and thus be of prognostic importance. Since MUC4 expression has been shown to increase progressively in precancerous pancreatic neoplasias[36], the presence or absence of CPC MUC4 expression may be used for risk stratification of patients with precancerous conditions.

Despite the fact that enumeration of CTCs has been shown to be a prognostic biomarker in a number of common cancers, CTC enumeration has not yet been incorporated into standard clinical practice in the management of any cancer.[38] However, the integration of genetic analysis in parallel with cell enumeration may allow for the development of stronger biomarkers and incorporation of these in clinical practice.[39] The genetic analysis of CPCs may reveal early signs of pancreatic carcinogenesis, before any cancer is clinically observable, without requiring an invasive biopsy. Moving beyond CTC enumeration, genetic analysis can provide information about prognosis and disease progression. Genetic mutations in circulating cell populations have shown to be prognostic of treatment outcome in lung cancer.[39] The technical difficulty associated with genotyping circulating cells is considerable, owing to their rarity and the presence of contaminating wild-type genetic material. Point mutations in circulating cell have been analyzed using mutation-specific qPCR[39]. A drawback of this approach is that it relies on the recognition of known SNPs using mutation-specific primers. As an alternative to genetic analysis, a mutational protein-level approach has recently been described, using an antibody specific to a mutated protein in the lysate from circulating cells.[15] However, this methodology relies on the availability of mutation-specific antibodies, only available for a subset of SNPs. Direct genetic sequencing represents the gold standard for genotyping and requires no previous knowledge of the particular mutation of interest. However, direct sequencing is sensitive to the presence of wild-type genetic material in the sample and can only be used in samples of high purity, i.e. if the number of mutated molecules is comparable to number of the wild-type molecules. In this respect, RNA level analysis may be more feasible than genomic level analysis as the mRNA copynumber of upregulated oncogenes, such as KRAS, can be assumed to be significantly higher in cancer cells compared to the wild-type cells.

Activating KRAS mutations represent some of the most common mutations in human carcinomas.[40] The KRAS gene encodes a small GTPase signaling protein that plays a fundamental role in cell growth regulation. KRAS mutations are found in more than 85% of patients with PC and in approximately 80% of patients with high-risk precancerous cystic lesions.[40] The molecular profiles of activating KRAS mutations are well described and a vast majority of mutations occur in codon 12 and 13 of the KRAS gene[41], which makes them suitable for analysis with RT-PCR-based amplification followed by genetic sequencing.

We have developed a microfluidic platform optimized to capture, identify and genotype CPCs, building on our previously described Geometrically Enhanced Differential Immunocapture (GEDI) device.[18 11 12] In this platform we explore capture chemistry as a design parameter and study its influence on the phenotype of captured cells. Our platform uses a combination of anti-EpCAM and anti-hMUC1 capture and allows for the release of intact cell nuclei and downstream KRAS oncogene genotyping.

Materials and methods

Device fabrication and functionalization

Devices were fabricated by A.M. Fitzgerald & Associates (Burlingame, CA) according to previously described specifications[11 18]. The silicon device surfaces were functionalized with NeutrAvidin (Thermo Fisher Scientific, Rockford, IL) with a previously described protocol[18]. The devices were functionalized with primary antibodies via biotinylated secondary linker antibodies. NeutrAvidin functionalized devices were (1) incubated with 10 μg/ml biotinylated goat anti-mouse antibody (Santa Cruz Biotechnology, Dallas, TX) and (2) incubated with either 10 μg/ml anti-EpCAM antibody (Clone 158206, R&D Systems, Minneapolis, MN), 10 μg/ml anti-MUC1 antibody (AR20.5) or 5 μg/ml anti-EpCAM and 5 μg/ml anti-MUC1 antibody. Control devices were functionalized with biotinylated normal (non-specific) mouse antibodies (Santa Cruz Biotechnology). All antibodies were prepared in 1% BSA in PBS.

Cell culture

Cell lines (Capan-1, PANC-1 and BxPC-3) were obtained from ATCC (Manassas, VA). All cell lines were cultured in humidified incubators (37 °C and 5% CO_2) using media recommended by ATCC (Capan-1: 20% FBS IMDM, PANC-1: 10% FBS DMEM and BxPC-3: 10% FBS RPMI) and 1X penicillin/streptomycin. Cells were used only below passage number 30 and cells were harvested after 4-6 days of culture at 60-80% confluency.

Lab on a Chip Accepted Manuscript

Quantitative flow cytometry

Cells were trypsinized for 5-10 minutes at 37 °C and then fixed with the Foxp3 fixation/permeabilization kit (eBioscience, San Diego, CA). Staining was performed with 0.5μg primary antibody/10^6 cells and 0.2μg PE-conjugated secondary antibody/10^6 cells in blocking flow cytometry staining buffer (eBioscience). Analysis was performed on a LSRII flow cytometer (BD Biosciences, San Jose, CA) and PE-Quantibrite beads (BD Biosciences) were used to quantify the antibodies bound per cell (ABC) count for this staining protocol. Data processing and calculation of the ABC counts were performed with custom MATLAB software.

Capture experiments

Cells were trypsinized for 5-10 minutes at 37 °C, labelled with 2μg/ml Calcein AM (Santa Cruz Biotechnology) for 45 minutes and resuspended in carrier solution (1% BSA, 1 mM EDTA in PBS) at approximately 300 cells/ml. Peripheral blood mononuclear cells (PBMCs) were isolated from donor blood using Ficoll centrifugation, labelled with CellTracker orange (Invitrogen, Grand Island, NY) and resuspended at approximately 500 cells/ml. Functionalized silicon devices were mounted with Tygon tubing inlets and outlets in a PMMA holder. Cell capture was achieved by flowing 1 ml cell suspension through the device at 1 ml/h followed by manual cell enumeration using fluorescence microscopy.

Isolation of captured nuclei

Targeted cell membrane lysis and release of nuclei from captured cells was performed using overnight incubation with a modified NST buffer (117mM NaCl, 8 mM Tris base, 0.8mM $CaCl_2$, 38 mM $MgCl_2$, 0.04% BSA, 0.16% NP-40 surfactant in DI water) with and without DAPI (10μg/ml), based previously described method[42].

RNA sequencing

RT-PCR primers were designed to amplify a 249 bp fragment containing codon 12 of human KRAS using the NCBI primer-BLAST tool; forward: GGAGAGAGGCCTGCTGAAAA and reverse: CCCTCCCCAGTCCTCATGTA. The forward primer was designed to overlap on neighboring KRAS exons to increase the RNA specificity of the RT-PCR amplification. Calcein labelled Capan-1 cells were spiked in control blood at 300 cells per ml. The cells were captured using anti-EpCAM GEDI. After washing with PBS and cell enumeration, RNA was extracted directly on-chip using the RNEasy kit (Qiagen). Extracted RNA from whole blood and Capan-1 cells spiked in PBS served as wild type and positive controls respectively. RT-PCR of extracted RNA was performed using a single tube reaction and the recommended protocol (OneStep, Qiagen); reverse transcription 30 min at 50 °C, PCR activation 15 min at 95 °C, 35 cycles of denaturation 45 s at 94 °C, annealing at 45 s at 61 °C and extension 1 min at 72 °C, followed by final extension 10 min at 72 °C. Successful KRAS cDNA amplification was confirmed using agarose gel separation. RT-PCR products were treated with alkaline phosphatase and exonuclease (ExoSAP-IT, Affymetrix) to remove remaining primers from RT-PCR reaction. Sequencing of GEDI captured samples and whole blood controls was performed by the Cornell Life Sciences Core Facility on an automated 3730xl DNA analyzer (Invitrogen), using Big Dye terminator chemistry, the reverse primer used for RT-PCR as sequencing primer and AmpliTaq-FS DNA polymerase (Invitrogen)

Capture and staining of clinical samples

Blood was obtained through venipuncture of a patient with clinically confirmed pancreatic ductal adenocarcinoma (PDAC). 1ml blood was processed through GEDI devices functionalized with anti-EpCAM, anti-hMUC1 and anti-hMUC1/EpCAM antibodies. Samples were fixed in 2% PFA in 50% PHEM buffer (60 mM PIPES, 25 mM HEPES, 10 mM EGTA and 2 mM $MgCl_2$) for 15 minutes and blocked in 6% BSA and 10% normal goat serum in PBS for 1 hour. After staining of surface markers, the samples were permeabilized with 0.25% (w/w) Triton x-100. The samples were stained for MUC4 with a primary (ab60720; abcam, Cambridge, MA, USA) and an AlexaFluor 488 conjugated secondary antibody (Invitrogen), for CD45 with a Qdot-800 conjugated antibody (Invitrogen), for CK using a CF543 (Biotium, Hayward, CA, USA) conjugated anti-pan-CK antibody (C11; BioLegend, San Diego, CA, USA) and for DNA/nuclei using DAPI (Invitrogen). Samples were collected, processed, fixed and stained within 48h.

Clinical sample analysis

Stained samples were imaged using a Zeiss LSM Live Confocal Microscope (10x 0.3NA). All cell-sized DAPI+ events with brightness DAPI and CK barely above the background noise were identified using image processing in a custom MATLAB algorithm. The prescreened events were then classified as CPCs or non-CPCs using manual classification. DAPI+/CD45-/CK+, DAPI+/CD45-/MUC4+ and DAPI+/CD45-/CK+/MUC4+ were used as CPC criteria.

Results and discussion

Expression analysis in model cell lines

A panel of three PC cell lines (Capan-1, PANC-1 and BxPC-3) where used as models for CPCs in the development of the

Lab on a Chip Accepted Manuscript

This journal is © The Royal Society of Chemistry [year]

capture methodology. These cell lines represent cells isolated from both primary pancreatic tumors (PANC-1 and BxPC-3) and liver metastasis (Capan-1); cells in different states of differentiation: Capan-1 (well differentiated), BxPC-3 (moderately to poorly differentiated) and PANC-1 (poorly differentiated); and varying mutation status of key oncogenes (KRAS, TP53, CDKN2A/P16 and SMAD4)[43] as well as distinct levels of MUC1 expression[44].

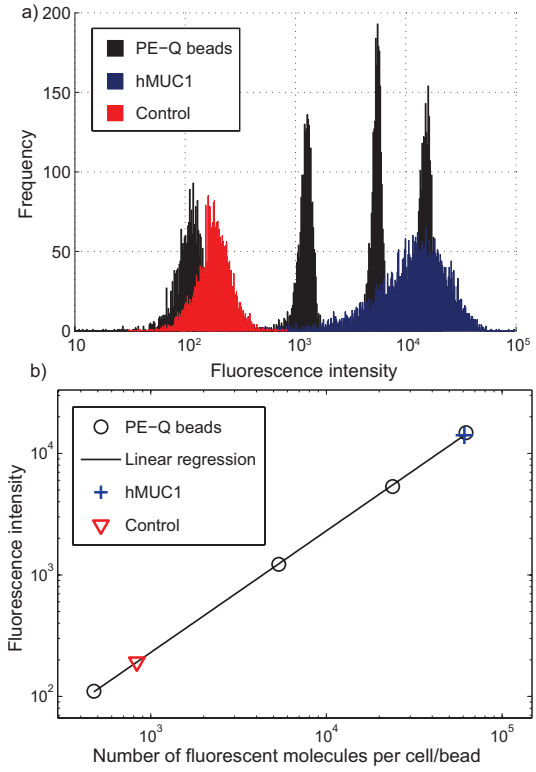

Fig. 1 Calibration of the antibody bound per cell (ABC) count for determination of antibody binding in PC cell lines, a) histogram showing gated flow cytometry data of phycoerythrin (PE) labelled Quantibrite beads of four intensity levels (black), Capan-1 cells stained with control (red) and hMUC1 (blue) antibodies a) calibration of the ABC count with PE-Quantibrite beads.

The expression level of EpCAM and hMUC1 was determined with quantitative flow cytometry for all three cell lines, as shown in Fig. 1. Quantitative flow cytometry determines the antibodies bound per cell (ABC) count of a population of cells calibrated using beads with known numbers of bound fluorescent molecules. Candidate antibodies for immunocapture were selected based on strong and consistent staining across all three cell lines. One anti-EpCAM (Clone 158206 mouse mAb, R&D) and one anti-hMUC1 (AR20.5[30] mouse mAb) antibody were identified as promising candidate antibodies for immunocapture. Fig. 2 shows the resulting ABC counts for these antibodies and cell lines. Since we ultimately aim to determine the influence of capture chemistry design on resulting phenotype of captured cells, the choice of model cell lines is important. In addition to the reasons mentioned above, the flow cytometry results show that this panel of cell lines displays a wide range of expression levels of EpCAM and hMUC1. In our experiments, Capan-1 cells displayed the strongest staining for both EpCAM and hMUC1 whereas PANC-1 stained the weakest for both, with ABC counts ranging from ~10,000 to ~70,000 for the three cell lines. Previous studies have reported EpCAM ABC counts in the range of 2,000 to 500,000 in a variety of cancer cell lines.[15] Interestingly, the relative hMUC1 ABC counts between cell lines do not correlate with previously described mRNA expression levels of these cell lines[44]. We attribute this difference to intrinsic differences in mRNA and surface antigen quantification, the specific fixation protocol used as well as differences in MUC1 glycosylation, accumulation and turn-over. Previous work has highlighted the utility of EpCAM capture[45] for immunocapture of CTCs from many carcinomas, but the role of MUC1 remains less clear. Cocktail capture has been presented in multiple contexts.[20] However, parallel anti-EpCAM/hMUC1 capture has not been implemented in microdevice technology to date and this strategy allows implementation of a novel capture modality in a new device.

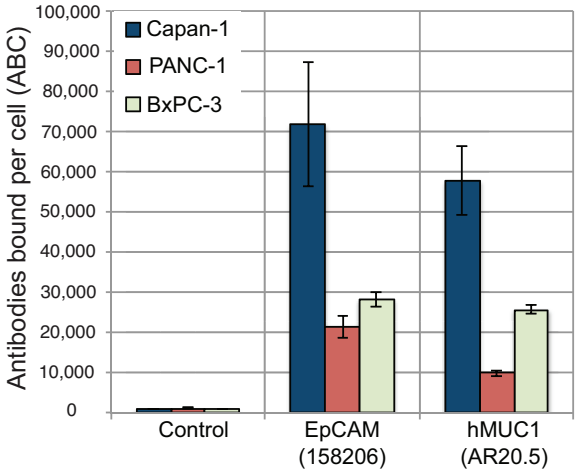

Fig. 2 Antibody bound per cell (ABC) counts for EpCAM, hMUC1 and PE labelled secondary control antibodies in cell lines Capan-1, PANC-1 and BxPC-3,

Microfluidic immunocapture of model cell lines

We have previously described the GEDI capture geometry in detail[18]. In short, the GEDI device[11 18 46] is a microfluidic

Lab on a Chip Accepted Manuscript

chip that captures rare cells from blood or cell suspensions, as shown in Fig. 3a. GEDI uses the combination of cancer-specific antibody immunocapture with a micropost geometry that maximizes the collision frequency between the substrate and larger cells (e.g., CTCs), and minimizes collisions of smaller contaminating cells (e.g. leukocytes). We have previously described the GEDI platform in a prostate [18,21], breast [19] and gastric [19] cancer context. We have shown how biotinylated antibodies can be functionalized onto NeutrAvidin coated silicon surfaces [18,21]. However, biotinyation of low concentration antibody samples requires high antibody purity and is typically inefficient. Biotinylated versions of primary antibodies are often not commercially available. As an alternative, we have here developed a protocol that attaches primary antibodies to silicon surfaces via biotinylated secondary antibody linkers, omitting any modification of the primary antibody. Fig. 3c shows a schematic of the functionalization chemistry used. Using this approach, we have implemented anti-EpCAM/hMUC1 modalities because of their importance in PC. We expect new anti-EpCAM/hMUC1 devices will enable investigation of questions regarding heterogeneity in CTCs in PC.

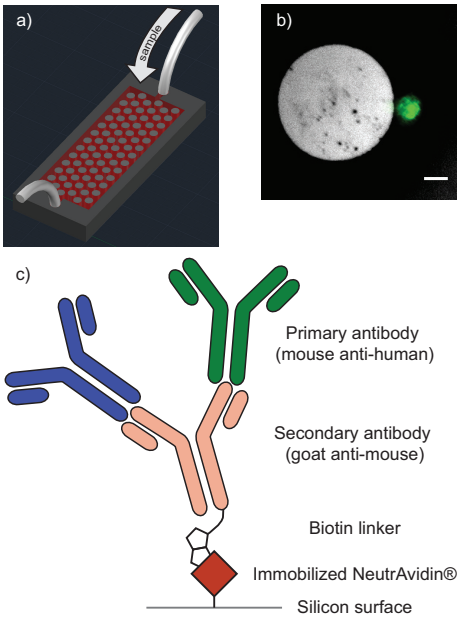

Fig. 3 a) schematic overview of the GEDI device, modified from Kirby *et al.* [18], microposts not to scale b) calcein-stained (green) PANC-1 cell captured on a GEDI micro post functionalized with a cancer-specific MUC1 antibody. Scale bar: 20 μm c) silicon surface functionalization with primary antibodies and secondary antibody linker chemistry that allows for multiple parallel capture antibodies.

To determine the efficiency of immunocapture in this system, fluorescently labelled cells were resuspended in buffer solution at physiologically relevant levels (300 cells/ml) and processed through GEDI devices, followed by manual counting. A representative image of a PANC-1 cell captured on GEDI micropost can be seen in Fig. 3b. We hypothesize that anti-hMUC1 capture alone or in combination with anti-EpCAM capture will will capture a more clinically relevant population of CPCs as compared to anti-EpCAM capture alone. To evaluate capture performance, we have determined the capture efficiency for all three scenarios, while ensuring that the total amount of antibody in the incubation solution was constant between experiments. As expected, anti-EpCAM alone resulted in efficient immunocapture while anti-hMUC1 capture alone resulted in lower capture efficiencies. However, a 1:1 antibody cocktail of anti-EpCAM and anti-hMUC1 performed indistinguishably from anti-EpCAM capture alone. Fig. 4a shows the resulting capture efficiencies from EpCAM, hMUC1 and EpCAM/hMUC1 cocktail capture. These results show that for these three cell lines, cocktail EpCAM/hMUC1 capture could replace the current EpCAM gold standard for immunocapure, without reducing capture efficiency. Furthermore, in a clinical scenario where EpCAM expression is reduced as a result of EMT while MUC1 expression is retained or upregulated, as is expected from clinical data [26], the capture performance of the EpCAM/hMUC1 cocktail may result in improved capture performance. Cocktail capture has been explored both for multiple epitopes on a single antigen [21] and for multiple antigens [20]. For single antigens, the data to date shows no synergy [21]. For multiple antigens, data to date shows potential to capture more of the heterogeneity expected in the CTC population [20]. However to our knowledge, no published study has thoroughly examined the effect of using multiple capture antibodies on the resulting capture efficiency as a function of cellular antigen expression level and cell size.

Our capture data show that Capan-1 and PANC-1 display EpCAM capture efficiencies more than twice that of BxPC-3, despite that fact that PANC-1 cells have lower EpCAM and hMUC1 ABC counts than the corresponding counts for Capan-1 and BxPC-3. This behavior can be explained by considering the size distribution of the cell populations and the predicted size-dependent performance of our device. [12] The predicted collision frequency and the experimentally observed capture efficiencies as function of cell size can be seen in Fig. 4b. Previously described simulations predict a sharp transition from low to high collision frequency for cells larger than 15μm [12]. We have measured the diameter of trypsinized populations of BxPC-3, Capan-1 and PANC-1 cells to be 13.3$\pm$2.9 μm,15.8$\pm$3.2 μm and 17.3$\pm$2.7 μm respectively. The majority of BxPC-3 cells will thus fall below the cutoff cell size of our device geometry, resulting in low collision rates and capture efficiencies lower than for the two cell lines with mean diameters larger than 15 μm. In the design regime of this

Lab on a Chip Accepted Manuscript

This journal is © The Royal Society of Chemistry [year]

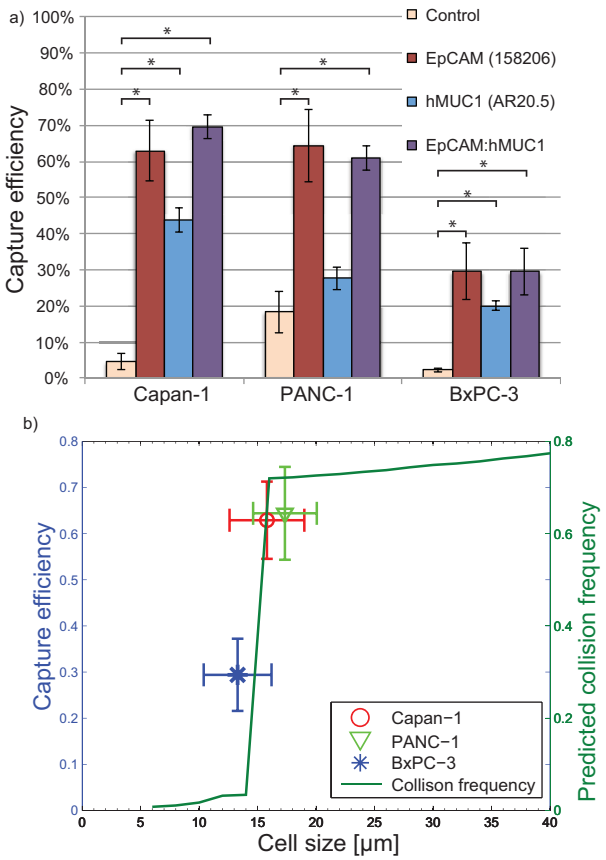

Fig. 4 a) GEDI microdevice immunocapture of Capan-1, PANC-1 and BxPC-3 cells by anti-EpCAM and anti-hMUC1 antibodies, and an anti-EpCAM/hMUC1 antibody cocktail, b) anti-EpCAM capture efficiencies of Capan-1, PANC-1 and BxPC-3 cells and predicted collision frequency as function of cell size, based on previously described simulations [12]. ∗ indicates statistically significant difference with p=0.05

platform, size dominates over relative levels of capture target expression provided that the cells express some minimum level of the capture target. Unlike staining for flow cytometry, for which antibodies are freely suspended in solution and can reach sterically obstructed epitopes through diffusion, antibodies for immunocapture are immobilized on surfaces allowing only for binding of epitopes that are pendant on the outer surface of the cell membrane. It is thus expected that some strongly staining antibodies will fail to result in efficient immunocapture. The resulting capture efficiency depends on the abundance and accessibility of antibody binding sites on the target cells. Since the saturation density of antibodies functionalized on the device surface is finite, the use of multiple capture antibodies reduces the surface density of each antibody type. In order for the addition of an additional parallel capture mode to increase capture efficiency, the gain in number and accessibility of possible capture targets has to outweigh the loss of capture efficiency that results of having fewer antibody molecules of each type on the surface. An example of a case where the addition of a second antibody leads to reduced capture efficiency can be seen in a previous capture study, conducted in a Hele-Shaw flow microdevice [21]. In that case, the second antibody was specific to a juxtamembranous epitope on the same target molecule as the first antibody. The total number of available target molecules thus remained unchanged with the addition of the second antibody, but the overall accessibility of binding sites was reduced, resulting in lower overall capture efficiency. In our case, the addition of a hMUC1 antibody to EpCAM capture increases the total number of available binding sites on each cell, as both EpCAM and hMUC1 are expressed strongly. The net result is that the overall capture efficiency for cocktail capture is retained as compared to anti-EpCAM and increased as compared to anti-hMUC1 capture alone. Given the natural variation in capture marker expression level between cells, the targeting of multiple highly-expressed capture targets will work to increase the robustness of capture to this intercellular variation. We thus conclude that a combined EpCAM and hMUC1 strategy has the potential to increase the robustness of capture to CPC heterogeneity and EMT, without reducing the overall capture efficiency as compared to the gold standard anti-EpCAM capture.

The most common source of cell contamination in microfluidic immunocapture devices is, due to their abundance as compared to rare circulating cells, the nonspecific adhesion of leukocytes [18]. Anti-EpCAM capture is widely used for immunocapture and results in only nonspecific adhesion of lekocytes. To ensure that the same is true for anti-hMUC capture, we conduced capture experiments using isolated donor peripheral blood mononucleated cells (PBMCs) in mixed populations with Capan-1 cells. The results showed that PMBCs adhered to our device at equal and negligible rates for both antibodies.

Isolation of captured cell nuclei

Recent studies have shown that breast cancer CTCs display genetic heterogeneity similar to that of primary and metastatic breast cancer tumors. [47] To analyze the heterogeneity within the CPC population single cell genetic analysis is required. To facilitate the future development of such a methodology we have developed a protocol for the release and isolation of single nuclei from captured cells on chip. Using targeted cell membrane lysis, followed by elution and retrieval of the nuclei through centrifugation, we have shown successful isolation of intact nuclei from captured cells. Examples of released and isolated nuclei can be seen in Fig. 5a.

Lab on a Chip Accepted Manuscript

Genetic analysis

Genetic analysis of captured CPCs is technically challenging due to the low number of cells present in blood and the presence of background wild-type genetic material from contaminating leukocytes. However, we have previously showed SNP detection of a mutated gene with amplified copynumber in captured cells, spiked in control blood[18]. To show ability to detect mutations in the important oncogene KRAS in small numbers of captured cells in the presence of a whole blood background, we used a PC cell line with known KRAS codon 12 mutation signature (Capan-1, GGT→GTT substitution) spiked in control blood. Calcein labelled cells were spiked in whole blood from a healthy donor (300 Capan-1 cells/ml control blood). RNA from captured cells was extracted directly on chip followed by RT-PCR and Sanger sequencing, the resulting KRAS codon 12 RT-PCR amplicons and Sanger sequences from 250 anti-EpCAM captured Capan-1 cells spiked in blood and buffer as well as whole blood wild type control are shown in Fig. 5b and c. RNA from whole blood showed no evidence of KRAS mutations while RNA extracted on chip from Capan-1 cells captured in buffer and whole blood revealed the expected GGT→GTT SNP in codon 12 of KRAS. In summary, these experiments show our ability to retrieve, amplify and analyze the genetic information from a very small number (<300) of captured cells even in the presence of contaminating wild-type genetic material.

Analysis of clinical samples

To show technical capability of capturing CPCs from clinical samples, we analyzed the blood from a patient with clinically confirmed pancreatic ductal adenocarcinoma (PDAC) using anti-EpCAM, anti-hMUC1 and cocktail anti-EpCAM-hMUC1 capture. After processing through the GEDI devices, the samples were fixed and stained. DAPI staining was used to indicate cell nucleus and CD45 antigen staining was used to identify and reject leukocytes, as previously described.[18] All samples were stained for both CK and MUC4.

Nuclear-like DAPI+ events were identified with an automated algorithm. Remaining events were classified manually with CD45-/CK+ and/or CD45-/MUC4+ as CPC criteria, resulting in between 102 and 165 events identified as likely CPCs per milliliter blood in this sample. Fig. 6 shows that, in this patient sample, events identified as likely CPCs from devices functionalized with anti-hMUC1 and anti-EpCAM/hMUC1 cocktail capture show increased MUC4 to CK intensity ratios relative to anti-EpCAM capture alone. This indicates that, in this sample, anti-hMUC1 capture results in capture of a cell population that is positive for both CK and MUC4. It is possible that this DAPI+/CD45-/MUC4+/CK+ cell population is of important clinical significance as MUC4 expression correlates with PC progression. Data from this

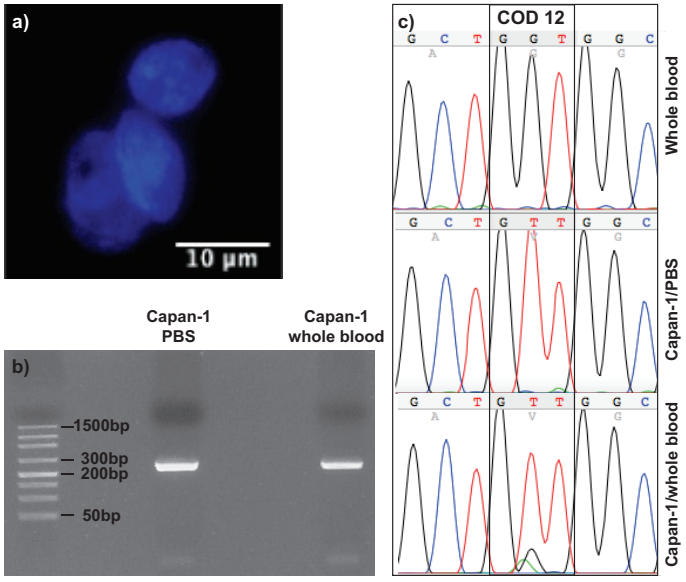

Fig. 5 a) released and isolated DAPI-stained (blue) Capan-1 nuclei, b) agarose gel with a 249 bp Capan-1 KRAS RT-PCR product from cells spiked in PBS buffer and whole blood, c) Sanger sequencing of the KRAS codon 12 RT-PCR product from whole blood, Capan-1 cells spiked in PBS and Capan-1 cells spiked in whole blood. The whole blood sequence shows the wild type codon 12 genotype (GGT) while RNA extracted from Capan-1 cells spiked in PBS and whole blood show the expected GGT→GTT oncogenic SNP. Note the presence of a small wild-type peak in the spiked blood sample. The presented sense sequences have been converted from anti-sense sequences generated by the Sanger sequencing reaction

sample shows that the apparent heterogeneity of the captured CPCs, as measured by the range of MUC4 staining in the captured CPCs, is larger in the anti-hMUC1 and EpCAM/hMUC1 samples than in the anti-EpCAM sample. Using this semi-automated approach to image analysis, we generate data suitable for clinical hypothesis generation. The resulting data can be gated and visualized like flow cytometry data and the phenotype of individual cells, as well as cell populations and subpopulations can be analyzed. The automated pre-screening of CPC events also greatly reduces the time and labor required for manual classification.

Conclusions

We have demonstrated a novel microfluidic platform for the capture and analysis of circulating pancreatic cells. This platform builds on a previously described geometry but incorporates novel anti-hypoglycosylated mucin 1 capture chemistry and explores parallelized EpCAM/hMUC1 capture as a novel capture paradigm. We show that a combination of anti-EpCAM and anti-hypoglycosylated mucin 1 capture per-

Lab on a Chip Accepted Manuscript

This journal is © The Royal Society of Chemistry [year]

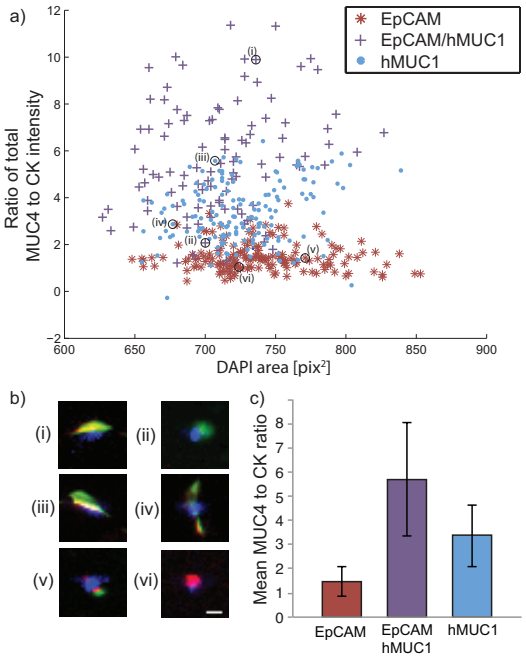

Fig. 6 Analysis of CPCs from a clinical PDAC patient sample, processed using anti-EpCAM, anti-EpCAM/hMUC1 and anti-hMUC1 GEDI devices, a) ratio of total MUC4 and CK staining intensity versus nuclear DAPI area in events classified as likely CPCs, b) inset images showing representative CPC events, i-ii anti-EpCAM/hMUC1 cocktail capture, iii-iv anti-hMUC1 capture and v-vi anti-EpCAM capture, images i,iii and iv are consistent with cells spread on microposts, DAPI (blue), cytokeratin (red), MUC4 (green). Scale bar: 10 μm c) mean MUC4-to-CK total intensity ratios for all three capture modes, error bars indicate standard deviation within the population of identified CPCs

forms as well as anti-EpCAM capture alone in model cell lines, while potentially increasing the robustness to variations in marker expression and EMT. To allow for the development of single-cell genetic analysis of circulating cells, we show release and isolation of single nuclei from captured cells. Using on-chip RNA extraction, RT-PCR and Sanger sequencing, we detected a known oncogenic KRAS SNP mutation in captured cells spiked in whole blood. We have also developed a staining protocol for clinical samples what involves standard circulating tumor cell makers, such as DAPI, CD45 and cytokeratin as well the PC-specific marker mucin 4. In an initial clinical sample, cocktail capture resulted in the capture of a cell population distinct from anti-EpCAM capture. Our approach allows for analysis of single cells and cell populations from patient samples and is suitable for clinical hypothesis generation. In all, we have shown feasibility of this platform for future evaluation in a clinical setting.

Acknoledgements

The work described was supported by the Cornell Center on the Microenvironment & Metastasis through Award Number U54CA143876 from the National Cancer Institute, the HHMI med-into-grad scholarship (FIT), the Lester and Sheila Robbins Scandinavian Graduate Student Fellowship (FIT), a National Science Foundation Graduate Research Fellowship under Grant No. DGE-1144153 (TBL), Early Detection Research Network U01 CA111294 (MAH), SPORE P50 CA 127297 (MAH), R01 CA057362 (MAH), K08DK088945 from the NIDDK (ADR) and a Career Development Award from the Pancreatic Cancer Action Network and American Association for Cancer Research (ADR)

References

1 T. Riall, W. Nealon, J. Goodwin, D. Zhang, Y. Kuo, C. Townsend and J. Freeman, *Journal of Gastrointestinal Surgery*, 2006, **10**, 1212–1224.
2 R. Pannala, A. Basu, G. M. Petersen and S. T. Chari, *The Lancet Oncology*, 2009, **10**, 88–95.
3 S. Maheswaran and D. A. Haber, *Current opinion in genetics & development*, 2010, **20**, 96–99.
4 V. Zieglschmid, C. Hollmann and O. Böcher, *Critical Reviews in Clinical Laboratory Sciences*, 2005.
5 E. Racila, D. Euhus, A. J. Weiss, C. Rao, J. McConnell, L. W. M. M. Terstappen and J. W. Uhr, *Proceedings of the National Academy of Sciences of the United States of America*, 1998.
6 A. D. Rhim, E. T. Mirek, N. M. Aiello, A. Maitra, J. M. Bailey, F. McAllister, M. Reichert, G. L. Beatty, A. K. Rustgi, R. H. Vonderheide, S. D. Leach and B. Z. Stanger, *Cell*, 2012, **148**, 349–361.
7 A. D. Rhim, F. I. Thege, S. M. Santana, T. B. Lannin, T. N. Saha, S. Tsai, L. R. Maggs, M. L. Kochman, G. G. Ginsberg, J. G. Lieb, V. Chandrasekhara, J. A. Drebin, N. Ahmad, Y.-X. Yang, B. J. Kirby and B. Z. Stanger, *YGAST*, 2013, 1–19.
8 D. R. Parkinson, N. Dracopoli, B. G. Petty, C. Compton, M. Cristofanilli, A. Deisseroth, D. F. Hayes, G. Kapke, P. Kumar, J. S. Lee, M. C. Liu, R. McCormack, S. Mikulski, L. Nagahara, K. Pantel, S. Pearson-White, E. A. Punnoose, L. T. Roadcap, A. E. Schade, H. I. Scher, C. C. Sigman and G. J. Kelloff, *Journal of Translational Medicine*, 2012, **10**, 1–1.
9 E. D. Pratt, C. Huang, B. G. Hawkins, J. P. Gleghorn and B. J. Kirby, *Chemical Engineering Science*, 2010, **66**, 1508–1522.
10 S. Nagrath, L. V. Sequist, S. Maheswaran, D. W. Bell, D. Irimia, L. Ulkus, M. R. Smith, E. L. Kwak, S. Digumarthy, A. Muzikansky, P. Ryan, U. J. Balis, R. G. Tompkins, D. A. Haber and M. Toner, *Nature*, 2007, **450**, 1235–1239.
11 J. P. Gleghorn, E. D. Pratt, D. Denning, H. Liu, N. H. Bander, S. T. Tagawa, D. M. Nanus, P. A. Giannakakou and B. J. Kirby, *Lab on a Chip*, 2010, **10**, 27.
12 J. P. Smith, T. B. Lannin, Y. A. Syed, S. M. Santana and B. J. Kirby, *Biomedical Microdevices*, 2013.
13 S. L. Stott, C.-H. Hsu, D. I. Tsukrov, M. Yu, D. T. Miyamoto, B. A. Waltman, S. M. Rothenberg, A. M. Shah, M. E. Smas, G. K. Korir, F. P. Floyd, A. J. Gilman, J. B. Lord, D. Winokur, S. Springer, D. Irimia, S. Nagrath, L. V. Sequist, R. J. Lee, K. J. Isselbacher, S. Maheswaran, D. A. Haber and M. Toner, *Proceedings of the National Academy of Sciences of the United States of America*, 2010.
14 S. Zheng, H. Lin, J.-Q. Liu, M. Balic, R. Datar, R. J. Cote and Y.-C. Tai, *Journal of Chromatography A*, 2007, **1162**, 154–161.
15 C. M. Earhart, C. E. Hughes, R. S. Gaster, C. C. Ooi, R. J. Wilson, L. Y.

Lab on a Chip Accepted Manuscript

Zhou, E. W. Humke, L. Xu, D. J. Wong, S. B. Willingham, E. J. Schwartz, I. L. Weissman, S. S. Jeffrey, J. W. Neal, R. Rohatgi, H. A. Wakelee and S. X. Wang, *Lab on a Chip*, 2014.

16 A. H. Talasaz, A. A. Powell, D. E. Huber, J. G. Berbee, K.-H. Roh, W. Yu, W. Xiao, M. M. Davis, R. F. Pease and M. N. Mindrinos, *Proceedings of the National Academy of Sciences*, 2009, **106**, 3970–3975.

17 E. Sollier, D. E. Go, J. Che, D. R. Gossett, S. O'Byrne, W. M. Weaver, N. Kummer, M. Rettig, J. Goldman, N. Nickols, S. McCloskey, R. P. Kulkarni and D. Di Carlo, *Lab on a Chip*, 2013, **14**, 63.

18 B. J. Kirby, M. Jodari, M. S. Loftus, G. Gakhar, E. D. Pratt, C. Chanel-Vos, J. P. Gleghorn, S. M. Santana, H. Liu, J. P. Smith, V. N. Navarro, S. T. Tagawa, N. H. Bander, D. M. Nanus and P. Giannakakou, *PLoS ONE*, 2012, **7**, e35976.

19 G. Galletti, M. S. Sung, L. T. Vahdat, M. A. Shah, S. M. Santana, G. Altavilla, B. J. Kirby and P. Giannakakou, *Lab on a Chip*, 2014.

20 M. Yu, A. Bardia, B. S. Wittner, S. L. Stott, M. E. Smas, D. T. Ting, S. J. Isakoff, J. C. Ciciliano, M. N. Wells, A. M. Shah, K. F. Concannon, M. C. Donaldson, L. V. Sequist, E. Brachtel, D. Sgroi, J. Baselga, S. Ramaswamy, M. Toner, D. A. Haber and S. Maheswaran, *Science*, 2013, **339**, 580–584.

21 S. M. Santana, H. Liu, N. H. Bander, J. P. Gleghorn and B. J. Kirby, *Biomedical Microdevices*, 2011, **14**, 401–407.

22 S. L. Stott, R. J. Lee, S. Nagrath, M. Yu, D. T. Miyamoto, L. Ulkus, E. J. Inserra, M. Ulman, S. Springer, Z. Nakamura, A. L. Moore, D. I. Tsukrov, M. E. Kempner, D. M. Dahl, C. L. Wu, A. J. Iafrate, M. R. Smith, R. G. Tompkins, L. V. Sequist, M. Toner, D. A. Haber and S. Maheswaran, *Science Translational Medicine*, 2010, **2**, 25ra23–25ra23.

23 S. A. Mani, W. Guo, M. J. Liao, E. N. Eaton and A. Ayyanan, *Cell*, 2008.

24 K. Polyak and R. A. Weinberg, *Nature Reviews Cancer*, 2009, **9**, 265–273.

25 M. A. Hollingsworth and B. J. Swanson, *Nature Reviews Cancer*, 2004, **4**, 45–60.

26 K. Nagata, M. Horinouchi, M. Saitou, M. Higashi, M. Nomoto, M. Goto and S. Yonezawa, *Journal of Hepato-Biliary-Pancreatic Surgery*, 2007, **14**, 243–254.

27 L. D. Roy, M. Sahraei, D. B. Subramani, D. Besmer, S. Nath, T. L. Tinder, E. Bajaj, K. Shanmugam, Y. Y. Lee, S. I. L. Hwang, S. J. Gendler and P. Mukherjee, *Oncogene*, 2010, **30**, 1449–1459.

28 B. P. Negin, N. J. Meropol and R. K. Alpaugh, *ASCO Meeting Abstract*, 2010.

29 N. Remmers, J. M. Anderson, E. M. Linde, D. J. DiMaio, A. J. Lazenby, H. H. Wandall, U. Mandel, H. Clausen, F. Yu and M. A. Hollingsworth, *Clinical Cancer Research*, 2013, **19**, 1981–1993.

30 W. Qi, B. C. Schultes, D. Liu, M. Kuzma, W. Decker and R. Madiyalakan, *Hybridoma and hybridomics*, 2001, **20**, 313–324.

31 R. Singh and D. Bandyopadhyay, *Cancer biology & therapy*, 2007, **6**, 481–486.

32 Y. Geng, T. Takatani, K. Yeh, J.-W. Hsu and M. R. King, *Cellular and Molecular Bioengineering*, 2013, **6**, 148–159.

33 B. Agrawal, M. J. Krantz, J. Parker and B. M. Longenecker, *Cancer Research*, 1998, **58**, 4079–4081.

34 I. Correa, T. Plunkett, A. Vlad, A. Mungul, J. Candelora Kettel, J. M. Burchell, J. Taylor papadimitriou and O. J. Finn, *Immunology*, 2003, **108**, 32–41.

35 A. Gradilone, C. Raimondi, C. Nicolazzo, A. Petracca, O. Gandini, B. Vincenzi, G. Naso, A. M. Aglianò, E. Cortesi and P. Gazzaniga, *Journal of Cellular and Molecular Medicine*, 2011, **15**, 1066–1070.

36 M. J. Swartz, S. K. Batra, G. C. Varshney, M. A. Hollingsworth, C. J. Yeo, J. L. Cameron, R. E. Wilentz, R. H. Hruban and P. Argani, *American journal of clinical pathology*, 2002, **117**, 791–796.

37 H.-U. Park, J.-W. Kim, G. E. Kim, H.-I. Bae, S. C. Crawley, S. C. Yang, J. R. Gum, S. K. Batra, K. Rousseau and D. M. Swallow, *Pancreas*, 2003, **26**, e48–e54.

38 C. Alix-Panabieres and K. Pantel, *Clinical chemistry*, 2013, **59**, 110–118.

39 S. Maheswaran, L. V. Sequist, S. Nagrath, L. Ulkus, B. Brannigan, C. V. Collura, E. Inserra, S. Diederichs, A. J. Iafrate, D. W. Bell, S. Digumarthy, A. Muzikansky, D. Irimia, J. Settleman, R. G. Tompkins, T. J. Lynch, M. Toner and D. A. Haber, *The New England journal of medicine*, 2008, **359**, 366–377.

40 J. WU, H. Matthaei, A. Maitra, M. Dal Molin, L. D. Wood, J. R. Eshleman, M. Goggins, M. I. Canto, R. D. Schulick, B. H. Edil, C. L. Wolfgang, A. P. Klein, L. A. Diaz, P. J. Allen, C. M. Schmidt, K. W. Kinzler, N. Papadopoulos, R. H. Hruban and B. Vogelstein, *Science Translational Medicine*, 2011, **3**, 92ra66–92ra66.

41 N. S. Pellegata, F. Sessa, B. Renault, M. Bonato, B. E. Leone, E. Solcia and G. N. Ranzani, *Cancer Research*, 1994.

42 N. Navin, J. Kendall, J. Troge, P. Andrews, L. Rodgers, J. McIndoo, K. Cook, A. Stepansky, D. Levy, D. Esposito, L. Muthuswamy, A. Krasnitz, W. R. McCombie, J. Hicks and M. Wigler, *Nature*, 2011, **472**, 90–94.

43 E. L. Deer, J. González-Hernández, J. D. Coursen, J. E. Shea, J. Ngatia, C. L. Scaife, M. A. Firpo and S. J. Mulvihill, *Pancreas*, 2010, **39**, 425–435.

44 M. A. Hollingsworth, J. M. Strawhecker, T. C. Caffrey and D. R. Mack, *International journal of cancer. Journal international du cancer*, 1994, **57**, 198–203.

45 W. J. Allard, *Clinical Cancer Research*, 2004, **10**, 6897–6904.

46 J. P. Smith, A. C. Barbati, S. M. Santana, J. P. Gleghorn and B. J. Kirby, *ELECTROPHORESIS*, 2012, **33**, 3133–3142.

47 A. A. Powell, A. H. Talasaz, H. Zhang, M. A. Coram, A. Reddy, G. Deng, M. L. Telli, R. H. Advani, R. W. Carlson, J. A. Mollick, S. Sheth, A. W. Kurian, J. M. Ford, F. E. Stockdale, S. R. Quake, R. F. Pease, M. N. Mindrinos, G. Bhanot, S. H. Dairkee, R. W. Davis and S. S. Jeffrey, *PLoS ONE*, 2012, **7**, e33788.

Lab on a Chip Accepted Manuscript

This journal is © The Royal Society of Chemistry [year]